

Article

Optimizing Recharge Area Delineation for Small- to Medium-Sized Groundwater Systems through Coupling Methods and Numerical Modeling: A Case Study of Linfen City, China

Kewei Lyu ¹, Qiulan Zhang ^{1,2}, Yali Cui ^{1,2}, Yaobin Zhang ¹, Yan Zhou ¹, Lu Lyu ³, Yihan Dong ^{1,*} and Jingli Shao ^{1,2,*}

¹ School of Water Resources and Environment, China University of Geosciences (Beijing), Beijing 100083, China; lvkewei107@163.com (K.L.); qlzhang919@cugb.edu.cn (Q.Z.); cuiyl@cugb.edu.cn (Y.C.); 3005190010@cugb.edu.cn (Y.Z.); yzhou@email.cugb.edu.cn (Y.Z.)

² MOE Key Laboratory of Groundwater Circulation and Environmental Evolution, China University of Geosciences (Beijing), Beijing 100083, China

³ The Third Geological Engineering Exploration Institute of Shanxi Province, Taiyuan 030620, China; lvlu325@163.com

* Correspondence: dongyihan101@163.com (Y.D.); jshao@cugb.edu.cn (J.S.); Tel.: +86-010-82323469 (J.S.)

Abstract: In previous investigations, the demarcation of capture zones within a specific research area predominantly relied on a singular method, leading to pronounced limitations and uncertainties. To address this challenge, an extensive field survey was conducted, focusing on the systematic classification of water sources in the Linfen City region. Building upon this classification, an intricate fusion of a hydrogeological analysis and formulaic methodology was employed. This integrated approach, coupled with independent numerical simulation methods, was applied to delineate recharge areas for both alluvial fan pore water in piedmont regions and exposed karst water in small- to medium-sized water sources. Simultaneously, precise spatial interpolation was carried out on water quality monitoring data from supply wells within the water source area for the year 2020. This meticulous analysis facilitated the determination of the spatial distribution characteristics of hydrochemical elements. To assess the water quality within the capture zone, the class III groundwater quality standards of China were employed as a pivotal tool for validating the results of the delineation of water source recharge areas. In the final analysis, a comparative study between the integrated coupling method and numerical simulation outcomes revealed the successful delineation of the boundaries for the water supply areas of Tumen and Caojiapo in Linfen City, covering areas of 5.5 km² and 22.29 km², respectively. Simultaneously, the combination of the three methods accurately outlined the boundary of the Hexi water supply area, encompassing an area of 2.5224 km². These results vividly illustrate that the amalgamation of various methodologies proves more beneficial for the precise delineation of capture zones, particularly in diverse types and scales of groundwater sources. The synergy exhibited by these three methods underscores their collective efficacy, providing a more comprehensive and intuitive delineation of the recharge areas for small- to medium-sized water sources. Consequently, these findings significantly enhance the practical application value of the study and hold promise in making substantial contributions to local groundwater security and management initiatives.

Keywords: capture zone; hydrogeological analysis method; formula method; numerical simulation; underground drinking water source recharge area



Citation: Lyu, K.; Zhang, Q.; Cui, Y.; Zhang, Y.; Zhou, Y.; Lyu, L.; Dong, Y.; Shao, J. Optimizing Recharge Area Delineation for Small- to Medium-Sized Groundwater Systems through Coupling Methods and Numerical Modeling: A Case Study of Linfen City, China. *Sustainability* **2024**, *16*, 1465. <https://doi.org/10.3390/su16041465>

Academic Editor: Fernando António Leal Pacheco

Received: 14 January 2024

Revised: 3 February 2024

Accepted: 5 February 2024

Published: 8 February 2024



Copyright: © 2024 by the authors. Licensee MDPI, Basel, Switzerland. This article is an open access article distributed under the terms and conditions of the Creative Commons Attribution (CC BY) license (<https://creativecommons.org/licenses/by/4.0/>).

1. Introduction

The capture zone represents the surrounding region of a drinking water supply well that contributes water to the well, with the overarching objective of maintaining chemical

concentrations in the extracted water below the prescribed drinking water standards. The underground drinking water supply recharge area encompasses the radial expanse of underground water that extraction wells can capture within water source zones. This includes the recharge area of the water source situated within the capture zone. In 2021, the Chinese government issued the “14th Five-Year Plan for Soil, Groundwater, and Rural Ecological Environment Protection,” with the explicit goal of fortifying the safeguarding of underground drinking water sources. This initiative entails the refinement of capture zone delineation and the promotion of recharge area delineation for shallow underground drinking water sources at the county level and beyond. The overarching aim is to enhance and preserve the quality of the groundwater environment, ensuring water environmental safety. The delineation of recharge areas serves the purpose of pinpointing primary sources of groundwater recharge and areas susceptible to potential pollution risks. This process facilitates a more profound comprehension of the radial regions of groundwater that extraction wells can capture, which proves vital for prognosticating shifts in the groundwater quality, sustaining water sources, and guaranteeing the enduring utilization of drinking water sources.

Various methodologies for delineating capture zones encompass empirical approaches, formulaic techniques, hydrogeological analyses, analytical procedures, and numerical simulation methods [1,2]. Empirical methods establish the capture zone radius through empirical parameters such as the renowned “50-day flow field iso-time lines” theory and the arbitrary radial distance determined by local hydrogeological conditions. The formulaic approaches, grounded in hydrological principles, adapt to diverse hydrogeological conditions by selecting characteristic parameters and calculating the capture zone radii using formulas. Notably, China’s “Technical Plan for the Division of Drinking Water Source Protection Areas” standardizes the formulaic methods for delineating capture zone radii in small- to medium-sized water sources, adjusting the recharge area based on aquifer characteristics and protected zones. In contrast, the United States typically employs a fixed-radius calculation method [3], assuming a circular capture zone. This method utilizes algebraic equations with parameters like the pumping rate and aquifer porosity, determining the wellhead capture zone radius based on the groundwater travel time from the circular edge to the wellhead. Despite its simplicity, this method’s high subjectivity and neglect of the factors affecting solute transport pose challenges, potentially resulting in capture zone accuracy discrepancies, either overestimating or underestimating them.

A hydrogeological analysis involves comprehensive analyses of the boundary types and properties of hydrogeological units within a water source area, including recharge runoff discharge conditions, to determine the recharge area range. This method necessitates significant professional expertise and precise hydrogeological survey data, requiring an understanding of the recharge and discharge conditions for hydrogeological units [4,5].

Analytical methods, particularly analytical element methods [6–11], provide profound insights into the fundamental physical processes governing the capture zone behavior, extent, and shape. These methods, devoid of numerical iteration, expedite computations compared to their numerical counterparts. Nevertheless, their applicability is constrained to regions characterized by relatively uncomplicated geological conditions, featuring simple geometric shapes, uniform permeability coefficients, a restricted number of elements, simplified boundary conditions, and steady-state scenarios.

In practical applications, numerical solutions prove invaluable for incorporating complex geological conditions into groundwater flow models. Numerical models utilize control equations to compute head values at specific time nodes and spatial discretization points, facilitating the calculation of transient, three-dimensional, heterogeneous anisotropic control equations under intricate geological conditions [12]. Traditional numerical methods for capture zone delineation encompass deterministic and probabilistic approaches, relying on aquifer property-associated travel times.

Deterministic methods delineate the capture zones by employing boundaries, with the widely used MODPATH numerical method [13] being a prominent choice. Reverse

particle tracking methods, involving the tracing of numerous particles along the flow direction, ascertain protection zone ranges based on fixed travel times [14–16]. Additional methods employing travel time include uniform flow equations [17], time of travel equations [18], and HYBRID methods [19]. Some advanced approaches such as MODPATH-OBS incorporate decay processes into particle tracking [20], while others consider convection, dispersion, adsorption, and first-order decay through the backward-in-time solution of the convection–dispersion equation [21–24]. Numerous studies underscore the substantial impacts of factors like transient flow, generalized source–sink terms, anisotropy, and horizontal–vertical conductivity on the protection zone size and shape [25–27]. For instance, a comparative analysis of wellhead protection areas (WHPA) under steady and transient conditions revealed that minor fluctuations caused by average seasonal changes result in a smaller capture zone range under steady conditions, prompting a 30% expansion. Considering transient factors in numerical models such as the groundwater flow direction, pumping rate, precipitation recharge, and hydraulic gradient allows for the comparison of WHPA and wellhead capture zone ranges at different scales. This approach advocates for redefining WHPA using time reliability and geological uncertainty [28].

Probability methods present capture zone ranges through probability graphs, with deterministic and probabilistic solute transport methods addressing pollution source identification and the propagation of capture zones within pumping wells. Stochastic simulation techniques are employed for delineating protection zone ranges, with conditional and unconditional Monte Carlo methods being widely utilized [29,30]. The strengths of probabilistic capture zone methods lie in their capacity to integrate uncertainty related to local-scale anisotropy into the delineation process, resulting in larger capture zone ranges than those determined by particle tracking methods [31,32]. Despite their potency, the utilization of solute transport equations based on convection–dispersion encounters computational burdens, limiting their historical adoption. Nevertheless, these methods remain instrumental in delineating protection zone ranges for a given travel time.

Recently, novel numerical models have emerged for capture zone delineation. The maximum concentration method (MaC-CZ), proposed by Okkonen et al., defines the capture zone ranges based on the maximum concentration rather than travel time, assuming a certain accuracy in estimating the pollutant concentration [33]. Addressing the limitations of existing methods in determining groundwater contribution areas associated with each source or sink, the dual delineation (DD) method introduced by Sbai (2018) stands as a distinct category. This Euler grid-based method not only delineates capture zones, but also provides a steady-state well capture zone, illustrating each well's contribution area to groundwater over infinite time. It emerges as a robust and effective alternative to particle tracking methods [34,35].

Past research often focused on employing a single method for capture zone delineation in specific study areas, neglecting consideration of the water source well type and recharge area. To mitigate the risk of drinking water source pollution and ensure the safety of underground drinking water sources, it becomes imperative to delineate a specific recharge area around capture zones.

Using Linfen City, Shanxi Province, China as an example, this study employs field surveys to classify water source types. Three delineation methods—hydrogeological analysis, formula method, and numerical simulation—are then employed to delineate the recharge areas for small- to medium-sized water sources, specifically alluvial fan-type porous water and exposed karst water. Simultaneously, water quality monitoring data from January to December 2020 are collected. GIS statistical calculation modules are utilized to determine the spatial distribution characteristics of chemical elements based on water source well monitoring data, enabling the assessment of the water quality within the capture zone range according to class III groundwater quality standards (in China). This research contributes to delineating the recharge areas for underground drinking water sources, ensuring the sustainable use of drinking water sources, water quality safety, and environmental health.

2. Materials and Methods

2.1. Study Area

Linfen City, situated downstream of the Fen River on the Loess Plateau in central Shanxi Province, China, encompasses a vast area of 2.02×10^4 km². The topography of Linfen City is predominantly characterized by undulating mountains and hills, featuring surface elevations ranging from 300 to 2500 m. The region experiences a continental semi-arid climate, with an average annual temperature fluctuating between 9.3 °C and 12.7 °C. Annual precipitation measures 495.9 mm, concentrated primarily from June to September. In contrast, the annual evaporation in the basin is substantial at 1763.2 mm. The hydrological dynamics are noteworthy, with seasonal flood runoff during the rainy season contributing to periodic floods, followed by dry conditions in the arid season.

The Tumen water source, nestled in the northwest of Linfen City and situated in the sloping expanse of Yershugou Village, Nanfen, Tumen Town, at the foothills of the Lüliang Mountains, holds strategic significance. Positioned east of the Luoyun Mountain fault zone, this water source boasts a surface elevation of 520 m, gradually diminishing from west to east. The western mountainous domain, recognized as the Longzici spring domain, predominantly comprises exposed rocks dating back to the Permian, Carboniferous, and Ordovician periods. The groundwater flow in this locale typically follows a west-to-east trajectory. In the water source area, the overall groundwater flow direction is from northwest to southeast, primarily facilitated by lateral flow from the Longzici spring domain through the permeable section south of the Tumen segment of the Luoyun Mountain fault. Under natural conditions, groundwater traverses eastward toward the Fen River valley, occasionally overflowing as springs in front of the alluvial fan. Presently, artificial extraction stands as the predominant method for groundwater discharge.

The Hexi water source, situated in the southern part of Linfen City and residing in the northern sloping plain of Chenguo Village, undergoes a fascinating transition from the mountain-front alluvial sloping plain to the alluvial plain of the Fen River. The source area exhibits a distinctive northwest–southeast distribution of loess hills formed by the Sanguanyu and Huoduyu streams originating from the mountainous areas of Xiangning County, ultimately flowing into the Fen River. Shallow groundwater in the water source area primarily undergoes recharge through lateral flow from the Longzici karst groundwater, atmospheric precipitation infiltration, and canal leakage. The natural movement of groundwater from west to east along the topography culminates in its discharge into the Fen River valley. Artificial extraction currently stands as the primary method for discharging both surface water and groundwater in the Fen River terrace region.

The Caojiapo water source, located in the southeast corner of Linfen City, unfolds against the backdrop of the loess hills' high loess tableland. It primarily taps into the concealed Ordovician karst groundwater in the uplift zone of the Danzi Mountain. The exposed rocks on the surface predominantly originate from the Quaternary alluvial layer, with a modest presence of exposed Ordovician and intrusive rocks. Influenced by the fault structure, the Ordovician limestone in the Danzi Mountain uplift zone has ascended, giving rise to well-developed fractures with robust water retention properties. The primary aquifer comprises Upper and Lower Majiagou Formation limestone, Baiyun limestone, and argillaceous Baiyun limestone. Groundwater recharge primarily occurs in the karst-exposed area and the covered area northeast of the water source, where the karst is exposed. Moreover, the thin cover of the Ordovician limestone in the covered area, coupled with the loose yellow soil layer and the semiconsolidated sand gravel layer of the third series above, enables the direct atmospheric precipitation recharge of the karst groundwater. The convergence of groundwater near the fractures of the Danzi Mountain uplift zone and its sides initiates a movement from the north and northeast to the south and southwest along the uplift zone and adjacent faults. The ultimate discharge point for karst groundwater is located in the spring domain outside the working area. In recent years, persistent groundwater extraction has precipitated a notable decline in the water table (Figures 1 and 2).

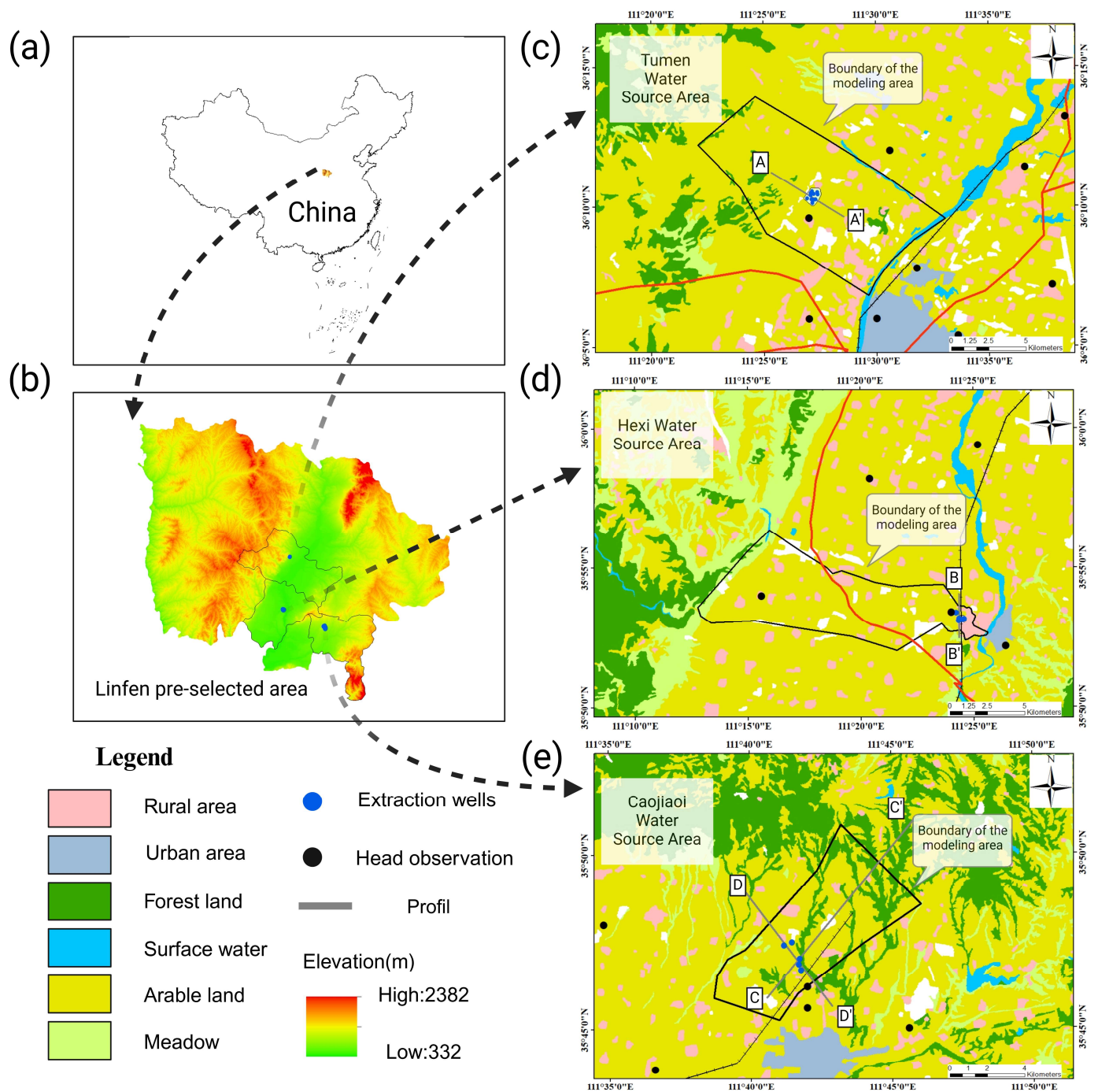


Figure 1. Location of the study area (a) within China (No. GS (2019) 1822) and (b) within the Linfen preselected area. (c) Details of the Tumen key site; (d) Details of the Hexi key site; (e) Details of the Caojiapo key site.

2.2. Methodology

In this scholarly inquiry, the delineation of recharge areas is methodically undertaken through the application of robust methodologies. The primary approaches employed encompass the empirical formula method, hydrogeological analysis—particularly through hydrogeological mapping—and numerical simulation. These strategies adhere to established protocols as outlined in authoritative references, specifically, the “Guidelines for Groundwater Pollution Simulation, Prediction, and Assessment” and the “Technical Guidelines for Delineating Recharge Areas of Underground Drinking Water Sources.”

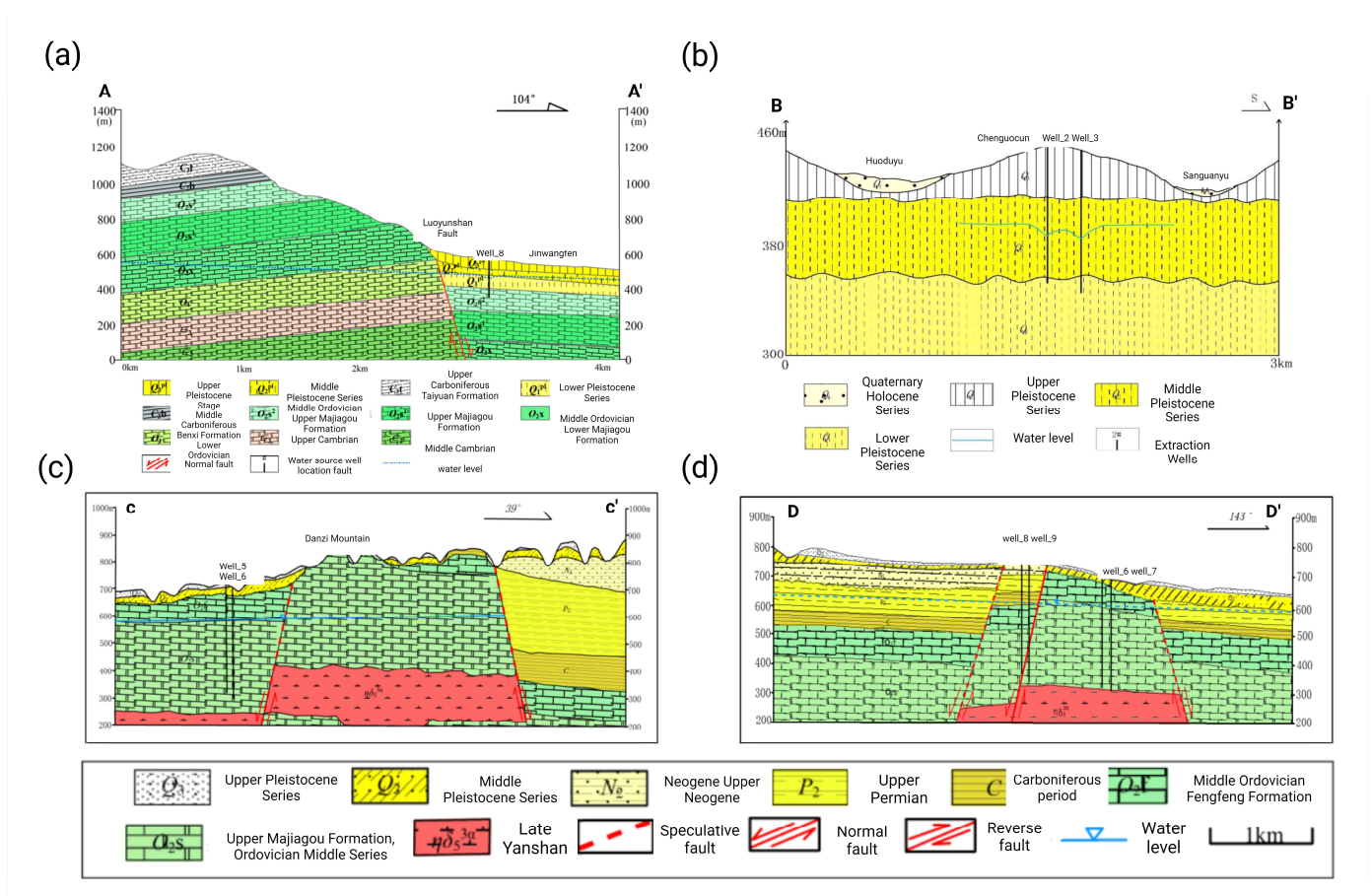


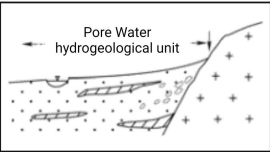
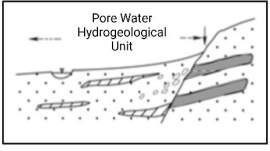
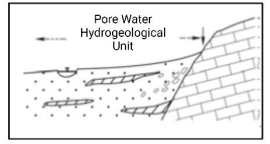
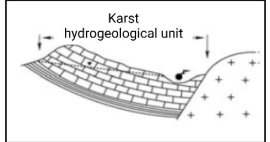
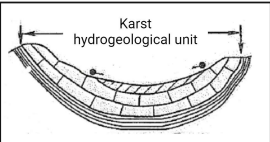
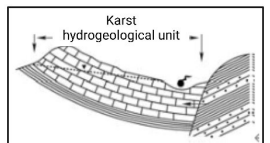
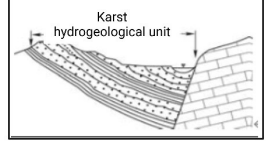
Figure 2. Study area profiles: (a) Tumen water source area profile; (b) Hexi water source area profile; (c) Caojiapo water source area, northwest–southeast direction profile; (d) Caojiapo water source area, southwest–northeast direction profile.

The elucidation of spatial distribution pertaining to the concentrations of chemical elements is achieved with precision through the adept utilization of geographic information system (GIS) statistical analysis modules. This analytical tool serves as an indispensable mechanism for validation, substantiating the accuracy and reliability of the delineation outcomes for recharge areas.

2.2.1. The Hydrogeological Analysis Method

The hydrogeological analysis method involves a meticulous exploration of the boundary types, characteristics, and recharge–discharge conditions within hydrogeological units to precisely identify the recharge area. The execution of this method requires a high level of expertise and the utilization of accurate hydrogeological survey data, emphasizing the need for a nuanced understanding of the recharge–discharge dynamics inherent in hydrogeological units. The categorization of hydrogeological unit boundaries includes impermeable, partially permeable, and permeable boundaries, each contributing distinct characteristics to the hydrogeological framework. A thorough elucidation of prevalent boundary types associated with hydrogeological units and the methodologies employed to delineate recharge area boundaries is meticulously presented in Table 1. This presentation emphasizes the critical importance of this analytical framework in comprehending the intricate hydrogeological dynamics, reinforcing its role in advancing our understanding of groundwater systems.

Table 1. Groundwater types and recharge area boundaries (modified from [36]).

Groundwater Type	Boundary Type and Characteristics	Recharge Area Boundary Definition	Cross-Sectional Illustration
Porous water	Impermeable boundary (outer side is impermeable rock layer)	Defined by this impermeable boundary; often occurs in areas where the porous water hydrogeological unit contacts impermeable bedrock	
	Partially permeable boundary (outer side is partially permeable rock layer)	Determined by the outer boundary of the permeable rock layer; frequently observed in regions with fractured structures	
	Permeable boundary (outer side is permeable rock layer)	Recharge area boundary is the outer impermeable boundary of the contact with the permeable rock layer; commonly found where the porous water hydrogeological unit meets permeable bedrock	
Karst water	Impermeable boundary: (a) continuous impermeable rock layer; (b) boundary consists of continuous impermeable fault or impervious rock layer	Area defined by the continuous impermeable layer; prevalent in basin topography, where the basin area is typically treated as a whole	
	Impermeable boundary: (a) continuous impermeable rock layer; (b) boundary consists of continuous impermeable fault or impervious rock layer	Defined by the impermeable fault or impervious rock layer	
	Partially permeable boundary (boundary consists of interleaved permeable and impermeable rock layers)	Determined by the outer impermeable boundary of the permeable rock layer; often found in areas with fractured structures	
	Permeable boundary (both hydrogeological units have a mutual boundary)	Recharge area boundary is the outer impermeable boundary in contact with the permeable rock layer	

2.2.2. Empirical Formula Method

The formulaic method, grounded in fundamental hydrological principles, adeptly accommodates the nuanced hydrogeological conditions observed across diverse regions. This method meticulously selects representative hydrogeological parameters and employs specialized formulas to compute protection zone radii. The inherent flexibility of this approach enables tailored adjustments in the shape and extension of the recharge areas, addressing the unique characteristics of various aquifers and water source types. This meticulous process culminates in the determination of an appropriately sized protection zone. However, it is crucial to emphasize that despite its apparent simplicity, this method is subjective and may overlook conditions related to solute transport, potentially leading to

the overestimation or underestimation of the protection zone intensity with insufficient precision [2].

Recognizing the intricate nuances of hydrogeological conditions and the inherent heterogeneity of aquifers, the demarcation of recharge area boundaries necessitates a segmented computational approach. The recommended formula for calculating recharge area boundaries is expressed as follows [36]:

$$R = \alpha \times K \times I \times \frac{T}{n_e} \quad (1)$$

where R is the computed length of the recharge area (m). α is the dimensionless coefficient, where $\alpha \geq 1$. K is the aquifer permeability (m/d). I is the hydraulic gradient (dimensionless). T is the migration time of groundwater points (d). n_e is the effective porosity of the aquifer (dimensionless).

It is crucial to note that when delineating recharge areas for water sources, the hydraulic gradient utilized should accurately reflect the maximum extraction rate, whether it be the current, standby, or planned rate. This meticulous consideration ensures a comprehensive and accurate representation of groundwater dynamics in the delineation process.

2.3. Groundwater Flow Model

2.3.1. Conceptual Model and Mathematical Model

In this investigation, we conducted simulation research on three critical water sources within the Yaodu District: Tumen, Hexi in Xiangfen County, and Caojiapo in Yicheng County. The simulated areas covered 97.5 km², 72 km², and 46.38 km², contributing to a comprehensive total area of 215.88 km². These water sources are associated with distinct aquifer types: Tumen and Hexi belong to the Quaternary, unconsolidated, porous confined aquifer, while Caojiapo is linked to the Ordovician, carbonate, fractured-karst confined aquifer.

Tumen water source: The topography of the Tumen water source area is demarcated by the Luo Yunshan fault to the west, exhibiting a gradual decrease in elevation from west to east, with the Fen River forming the eastern boundary. In terms of geological formations, the region is characterized by a significant thickness of Quaternary loose sediments, vertically divided into two aquifers: Q₃^{pl} constituting the first aquifer and Q₂^{pl} constituting the second aquifer. Within the model, the western side experiences lateral recharge from the mountain front, while the eastern side receives recharge through leakage from the Fen River. The upper layer of the model undergoes vertical recharge and discharge processes induced by precipitation and evaporation. Simultaneously, the bottom layer is designated as an impermeable boundary.

Hexi water source: The topography of the Hexi water source area is situated west of the Fen River, on the northern inclined plain fringe near Chenguo Village. The geological strata predominantly consist of a substantial thickness of Quaternary loose sediments, vertically partitioned into two aquifers: the first aquifer comprises Q₃^{pl}, and the second aquifer comprises Q₂^{pl}. Within the model framework, the eastern side is demarcated by the "Qiyi" canal as an impermeable boundary, while the western side receives recharge from Fen River leakage. The northern and southern boundaries receive leakage recharge from the tributaries of the Fen River, namely, Sanguanyu and Huodouyu. The upper layer of the model experiences vertical recharge and discharge processes induced by precipitation and evaporation, with the bottom layer serving as an impermeable boundary.

Caojiapo water source: The Caojiapo water source area's topography is characterized by two sets of northeast–southwest-oriented faults, causing the relative uplift of Mianshan and Danzishan, with terraces on both sides of the mountain front relatively descending. The eastern, northern, and three-sided regions are higher, while the central and southern parts are lower. Vertically, it is stratified into three aquifers: the first aquifer is the shallow aquifer composed of Quaternary pore water, and the second and third aquifers collectively constitute the deep aquifer, composed of limestone fissure karst water. In the model,

impermeable faults function as impermeable boundaries in the northern and southern regions, whereas the eastern and western regions are set as general head boundaries. The upper layer of the model undergoes vertical recharge and discharge processes induced by precipitation and evaporation, with the bottom layer serving as an impermeable boundary.

Given the conceptual hydrogeological models elucidated above and the inherent limitations in the available data, a generalization of the mathematical model of groundwater flow was necessitated. This generalization transformed the model into a homogeneous, isotropic, and steady-state, three-dimensional groundwater flow model, which was subsequently solved using appropriate boundary conditions.

$$\begin{cases} K\left(\frac{\partial^2 H}{\partial x^2} + \frac{\partial^2 H}{\partial y^2} + \frac{\partial^2 H}{\partial z^2}\right) + W - P - E = 0 & (x, y) \in \Omega, t \geq 0 \\ H(x, y, t)|_{t=0} = H_0(x, y) & (x, y) \in \Omega \\ H(x, y, t)|_{\Gamma_1} = \varphi_1(x, y, t) & (x, y) \in \Gamma_1, t \geq 0 \\ H(x, y, t)|_{\Gamma_2} = \varphi_2(x, y, t) & (x, y) \in \Gamma_2, t \geq 0 \end{cases} \quad (2)$$

In the equations provided [12], K represents the permeability coefficient of the confined aquifer in meters per day (m/d); H signifies the groundwater level in meters (m); W denotes the vertical recharge intensity (m/d); P denotes the pumping rate (m³/d); E represents the evaporation intensity (m/d); H_0 is the initial groundwater level (m); φ signifies the boundary water level (m); x and y represent the spatial coordinates (m); Ω is the computational domain; Γ_1 is the boundary associated with river conditions; and Γ_2 is the boundary associated with general head conditions.

This comprehensive modeling approach ensures a meticulous examination of groundwater dynamics, accounting for the intricate hydrogeological characteristics and boundary conditions specific to each water source.

2.3.2. Numerical Model

(1) Spatial discretization:

For the Tumen study area, a grid comprising 142 rows \times 182 columns was systematically generated, resulting in a total of 26,390 cells. The model configuration takes the form of a rectangular prism with specific dimensions: 142 rows \times 182 columns \times 2 layers.

The Hexi study area underwent meticulous partitioning into 53 rows \times 70 columns, yielding precisely 11,502 cells. The model structure, analogous to the Tumen study, is a rectangular prism with the following dimensions: 53 rows \times 70 columns \times 2 layers.

The Caojiapo study area was intricately segmented into 115 rows \times 122 columns, amassing a comprehensive total of 28,536 cells. The corresponding model structure assumes the form of a rectangular prism, featuring dimensions of 115 rows \times 122 columns \times 3 layers (Figure 3).

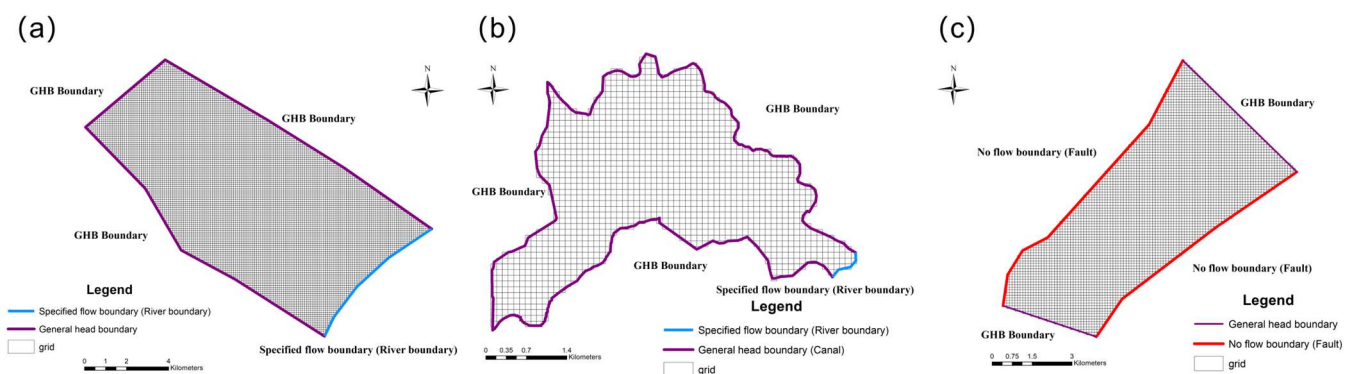


Figure 3. Schematic diagrams of grid division and boundary conditions in three study areas: (a) Tumen water source area; (b) Hexi water source area; (c) Caojiapo water source area.

When the grid division in the study area is too large, it leads to an overly coarse generalization of hydrogeological conditions, resulting in suboptimal outcomes. Conversely, an excessively fine grid division increases the grid count, imposing a burden on the efficiency of the model operation. The primary objective in establishing the numerical model is to delineate the capture zone using MODPATH particle tracking based on the foundation of the hydrological flow model. The three water source areas are all characterized as medium to small sized, with areas ranging from approximately 50 km² to 100 km². Opting for a 100 m grid facilitates an accurate delineation of the water source areas while maintaining computational efficiency. Furthermore, due to data acquisition constraints in the study area, precise correspondence between the digital elevation model (DEM) data and the grid is crucial. Therefore, the DEM data collected are converted to a 100 m resolution using QGIS and SWAP to ensure accurate alignment with the grid. The grid is subsequently divided into 100 m × 100 m cells, designating cells within the study area as active units and those outside as inactive units.

(2) Boundary and initial conditions:

Based on the shallow and deep aquifer flow field distribution map provided by the Shanxi project team for the Linfen Basin in January 2018, the spatial representation of the flow field is achieved by discretizing the lines into points. Through the interpolation of these discrete points, one can obtain the initial water level values for each cell in the aquifer. These initial water level values serve as the 'initial conditions for the model. Boundary conditions and source–sink terms encompass the treatment of atmospheric precipitation infiltration in the 'Recharge package. Evapotranspiration processes are addressed through the 'Evapotranspiration package for the discharge of water through evaporation. River discharge is managed through the 'Specified flow boundary, with the recharge volume determined based on the leakage of groundwater influenced by river flow rates. Lateral recharge from mountain fronts is handled using the 'General Head Boundary module, and the distribution of recharge volumes along the boundaries is contingent upon the location of outlet points from the mountainous terrain. In this study, we judiciously employed MODFLOW from the GMS 10.4 software package for numerical solution. The solution method adopts rectangular discretization and linear interpolation techniques, employing the finite difference method to seamlessly transform the mathematical model into a set of finite difference equations. Subsequently, building upon the outcomes of the hydrological model, the MODPATH reverse particle tracking module will be adroitly employed to delineate the recharge area. Noteworthy is the categorization of all water sources in the study area as medium to small, prompting the circumscription of the recharge area based on the first-level protection zone of the water source, defined by a 15-year, 1000-day (6475 days) flow path.

2.3.3. Model Calibration

Under conditions of steady state, an extensive calibration effort was initiated for the Tumen, Hexi, and Caojiapo water sources. This involved utilizing a dataset comprising 216 water level measurements collected from observation wells during the 2018–2019 period. Given limitations in existing geological–hydrological data, the initial reliance on empirical parameters from prior studies was deemed necessary. The calibration process encompassed manual trial and error, followed by refining relevant empirical parameters through the application of PEST software (in GMS 10.4). This approach facilitated the independent parameter estimation and uncertainty analysis, ensuring a robust alignment between simulation results and observed values. The correlation coefficients between groundwater level observations and simulation results for the three water sources were remarkably high at 0.93, 0.99, and 0.98, as illustrated in Figure 4, demonstrating an exceptional model fit.

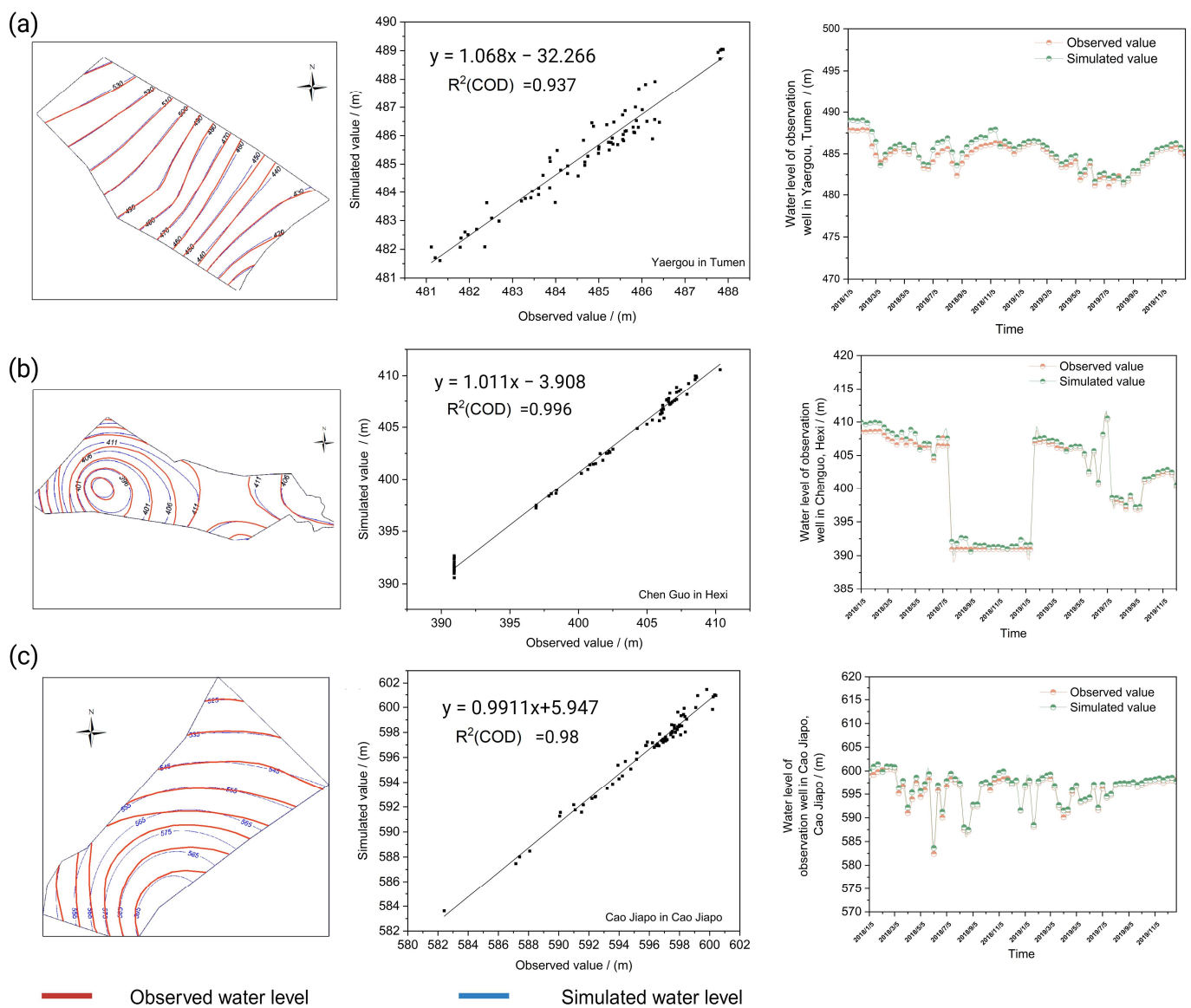


Figure 4. Head contours, correlation between simulated and observed groundwater levels, and comparison curve between observed water level and simulated water level. (a) Tumen water source area; (b) Hexi water source area; (c) Caojiapo water source area.

For steady-state models, the key performance indicators, including model bias, mean absolute error, and root mean square estimated error, were computed using the following formulas [37]:

$$\text{Bias} = \frac{1}{n} \sum_{i=1}^n (y_i - x_i) \quad (3)$$

$$\text{MAE} = \frac{1}{n} \sum_{i=1}^n |y_i - x_i| \quad (4)$$

$$\text{RMSE} = \sqrt{\frac{1}{n} \sum_{i=1}^n (y_i - x_i)^2} \quad (5)$$

where y represents the predicted value and x represents the observed value. In the Tumen water source area, the model bias is -0.06 m, the mean absolute error is 0.29 m, and the root mean square error is 0.34 m. In the Hexi water source area, the model bias is -0.049 m,

the mean absolute error is 0.16 m, and the root mean square error is 0.26 m. In the Caojiapo water source area, the model bias is 0.019 m, the mean absolute error is 0.42 m, and the root mean square error is 0.58 m.

In summary, the simulated groundwater flow field effectively aligns with the overall trend of the measured field, adeptly capturing the intricate, underground water flow patterns in the study area.

2.4. GIS Statistical Analysis to Validate the Defined Recharge Area

Drawing on field surveys and water quality monitoring, data spanning January to December 2020 were acquired within the operational zones of the Tumen, Hexi, and Caojiapo water sources. Sampling points, designated as supply wells for each water source, monitored 39 routine indicators (e.g., pH, TDS, SO_4^{2-} , and Cl^{2-}) monthly, with a comprehensive set of 93 indicators in July 2020 (including Be, B, 1,2-dichloroethane, 1,1,1-trichloroethane, etc.).

By leveraging the GIS geological statistical analysis module to conduct a statistical analysis of the sample test results, and subsequent to the Kruskal–Wallis test for all elements in Table 2, the existing water quality data underwent spatial interpolation to discern the spatial distribution characteristics of different parameters. Given the nonuniform distribution of water sample data within the study area, a geometrical interval was applied to classify the spatial interpolation results. This approach was adopted to obtain a more reasonable spatial distribution map of the chemical element concentrations. Based on the spatial distributions of representative chemical elements, the water quality was assessed using standards outlined in the “Standard for groundwater quality” (GB/T 14848-2017) [38] class III criteria (refer to Table 2). This comprehensive assessment served as supplementary validation for the defined recharge area.

Table 2. Statistical summary of the chemical compositions of groundwater samples from three water sources area and groundwater quality classification standards.

Parameter	Unit	Tumen Water Source Area ($n = 132$)				Standard for Groundwater Quality		
		Min	Max	Avg	SD	Class I	Class II	Class III
Total hardness (CaCO_3)	mg/L	338	457	412	28.156	≤ 150	≤ 300	≤ 450
TDS	mg/L	632	781	703	34.930	≤ 300	≤ 500	≤ 1000
SO_4^{2-}	mg/L	198	382	301	73.047	≤ 50	≤ 150	≤ 250
Cl^-	mg/L	11	30	17.542	5.373	≤ 50	≤ 150	≤ 250
$\text{NH}_4^+\text{-N}$	mg/L	0.02	0.127	0.044	0.032	≤ 0.02	≤ 0.10	≤ 0.50
F^-	mg/L	0.36	0.8	0.57	0.134	≤ 1.0	≤ 1.0	≤ 1.0
Parameter	Unit	Hexi Water Source Area ($n = 96$)				Standard for Groundwater Quality		
		Min	Max	Avg	SD	Class I	Class II	Class III
Total hardness (CaCO_3)	mg/L	449	591	514.125	30.981	≤ 150	≤ 300	≤ 450
TDS	mg/L	723	981	881.375	39.157	≤ 300	≤ 500	≤ 1000
SO_4^{2-}	mg/L	120	328	189.667	65.207	≤ 50	≤ 150	≤ 250
Cl^-	mg/L	80.7	164	96.592	17.339	≤ 50	≤ 150	≤ 250
$\text{NH}_4^+\text{-N}$	mg/L	0.025	0.13	0.042	0.030	≤ 0.02	≤ 0.10	≤ 0.50
F^-	mg/L	0.22	0.9	0.688	0.147	≤ 1.0	≤ 1.0	≤ 1.0

Table 2. Cont.

Parameter	Unit	Caojiapo Water Source Area (n = 72)				Standard for Groundwater Quality		
		Min	Max	Avg	SD	Class I	Class II	Class III
Total hardness (CaCO ₃)	mg/L	488	576	532.458	24.53	≤150	≤300	≤450
TDS	mg/L	1023	1458	1153.667	100.34	≤300	≤500	≤1000
SO ₄ ²⁻	mg/L	393	552	449.583	44.72	≤50	≤150	≤250
Cl ⁻	mg/L	55	70	62.5	3.46	≤50	≤150	≤250
NH ₄ ⁺ -N	mg/L	0.029	0.233	0.084	0.04	≤0.02	≤0.10	≤0.50
F ⁻	mg/L	1.1	1.5	1.258	0.13	≤1.0	≤1.0	≤1.0

Confidence interval 95%, $p < 0.05$. The significance of the grades was calculated with the Kruskal–Wallis test.

3. Results

3.1. Tumen Water Source Area Recharge Zone Division and GIS Statistical Analysis

In the delineation process, the initial step involves determining the runoff distance for the Tumen water source in the Yaodu District, situated proximately to loose deposits from the fourth series in front of the mountains. The closest distance to the water source well is 300 m, prompting an imperative assessment to determine if the 15-year runoff distance within the fourth series pores surpasses this minimum distance. If the runoff distance falls short of 300 m, the recharge area is delineated by the mountain front fault zone. In cases where the runoff distance exceeds 300 m, consideration is given to the exposure of bedrock in the mountain area, coupled with topography, to delineate the recharge area. The calculation process is expressed as $R = \alpha \times K \times I \times T/n_e$, with parameters derived from the literature [39] and empirical values: α , change coefficient (1.5); K , aquifer permeability (9.0 m/d); I , hydraulic gradient (6/1000); T , groundwater point migration time (6475 days); and n_e , effective porosity of the aquifer (0.3). The calculated R is determined to be 1748.2 m.

The subsequent geological structure analysis reveals that at the Jinwangfen location, the porous water level is lower than that of karst water in the mountain area. Without impeding impermeable bedrock at the fault, groundwater flows from west to east, recharged by karst water from the Ordovician limestone on the west side of the fault and receiving infiltration from atmospheric precipitation. The runoff recharges porous water on the east side of the fault. Considering the terrain, the upstream mountain slope exhibits a gradient of approximately 20.5° with three valleys. The drainage area of the valley region serves as the basis for delineating the recharge area, combined with a geological structure analysis, resulting in the final defined recharge area (Figure 5a).

The results of the numerical model division (Figure 5b) extend beyond the determined recharge area in the east–west direction compared to the formula and hydrogeological analysis. However, in the north–south direction, limitations in the boundary conditions may cause the numerical simulation results to yield a smaller recharge area than those determined by the formula and hydrogeological analysis. Despite these discrepancies, the overall trend of the numerical model's division aligns with the results from the formula and hydrogeological analysis. It is noteworthy that with more detailed data, further optimization of the simulation results is possible.

In summary, the Tumen water source employs the formula and hydrogeological analysis to define the recharge area, covering an area of 6.60 km², a perimeter of 10.288 km, and, after deducting the first-level protected area, a final recharge area of 5.5 km².

According to the 2020 Tumen water source water quality monitoring data, the groundwater monitoring indicators within the water source meet the standards for groundwater class III. Representative chemical elements, including the total hardness, sulfates, and fluorides from past studies with elevated levels, along with routine elements like total dissolved solids, chlorides, and ammonia nitrogen, were chosen for their spatial distribution analysis using GIS geological statistics (Figure 6).

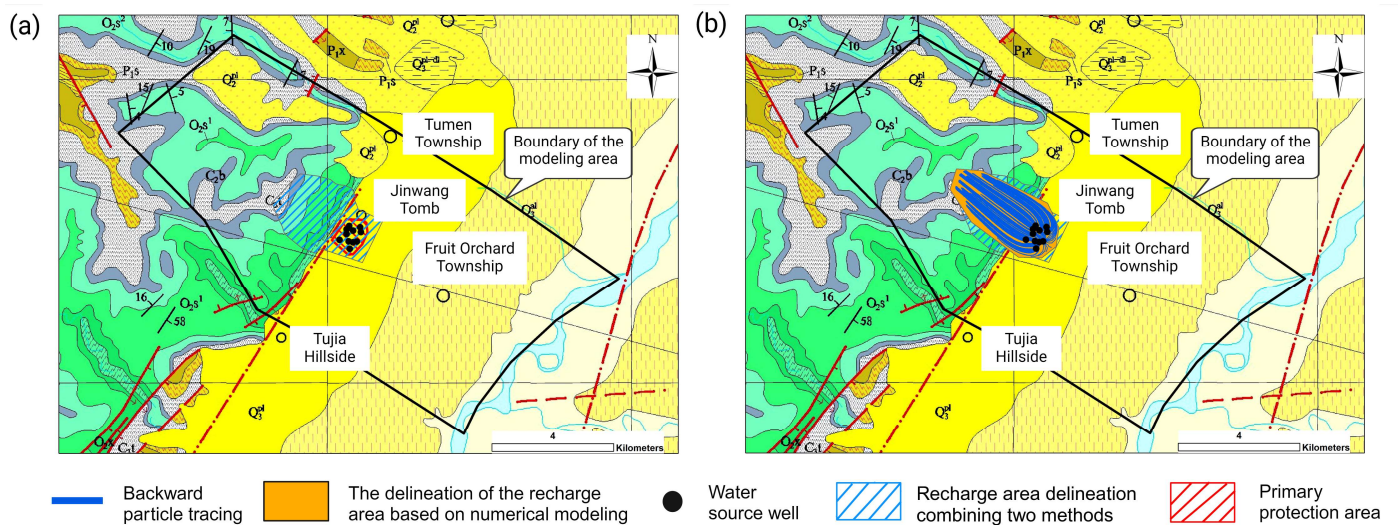


Figure 5. Groundwater recharge area of Tumen water source: (a) comparison of numerical simulation results with the results obtained from the first two methods; (b) recharge area boundaries defined by combining the two methods.

The groundwater chemical type in the water source area is $\text{SO}_4^{2-}\text{HCO}_3^- \text{Ca}\cdot\text{Mg}$ type, with total dissolved solids ranging from 632 to 781 mg/L, total hardness (as CaCO_3) from 338 to 457 mg/L, sulfates from 198 to 382 mg/L, chlorides from 11 to 30 mg/L, ammonia nitrogen from 0.02 to 0.127 mg/L, and fluorides from 0.36 to 0.8 mg/L. Due to differences in the groundwater storage conditions, circulation conditions, topography, geological structures, natural environmental background values, and human activities, the overall distribution of these chemical elements indicates higher values in the upper mountainous region and the riverfront region of the working area, whereas they are relatively lower around the delineated water source recharge area, suggesting good water quality. In conclusion, the GIS statistical results help validate the reasonability of the delineated recharge area for the water source.

3.2. Hexi Water Source Area Recharge Zone Division and GIS Statistical Analysis

To delineate the recharge area, the initial step involves calculating the runoff distance. By consulting the regional hydrogeological survey report and handbook of hydrogeology [40] for the study area, the average value for horizontal hydraulic conductivity (K) is determined to be 5.89 m/d. Considering a pumping test radius ranging from 160–200 m and n_e with a value of 0.22, the geological analysis indicates that the hydraulic gradient for the Hexi water source is smaller than that for the Houdong water source, registering at 0.004. Given Hexi's classification as a small- to medium-sized water source with the T set at 6475 days and a deliberately chosen, relatively high permeability coefficient, the safety factor α is set at 1.2. According to Formula (1), R is calculated as 832 m. Water source well 1, located at the westernmost edge near the recharge area, has a one-level protection zone radius of 92 m. The final determined upstream recharge area radius R for the water source is 924 m. Considering the pumping test's influence radius is 160–200 m, the downstream recharge area radius R is set at twice this radius to 400 m.

The Hexi water source is strategically positioned in the transitional zone between the mountain-front alluvial slope and the Fen River alluvial plain. The shallow groundwater in the mountain-front slope and the Fen River alluvial plain displays a network of various recharge pathways. In addition to receiving a lateral recharge from the bordering mountain, it undergoes an infiltration recharge from atmospheric precipitation, canal leakage recharge, irrigation percolation recharge, and reservoir leakage recharge. The overall discharge pattern of groundwater elegantly flows along the topography from west to east towards the Fen River valley, naturally revealing itself in the river valley. The secondary hydrogeological

unit area where the water source is located spans approximately 72 km². Combining this information with the hydrogeological analysis, the north and south boundaries of the recharge area are determined to be the lower-lying areas of Sanguanyu and Huoduyu. The western boundary is the mountain-front zone of the West Lvliang Mountain, serving as the primary recharge source for this hydrogeological unit, while the eastern boundary is demarcated by the Fen River (Figure 7a).

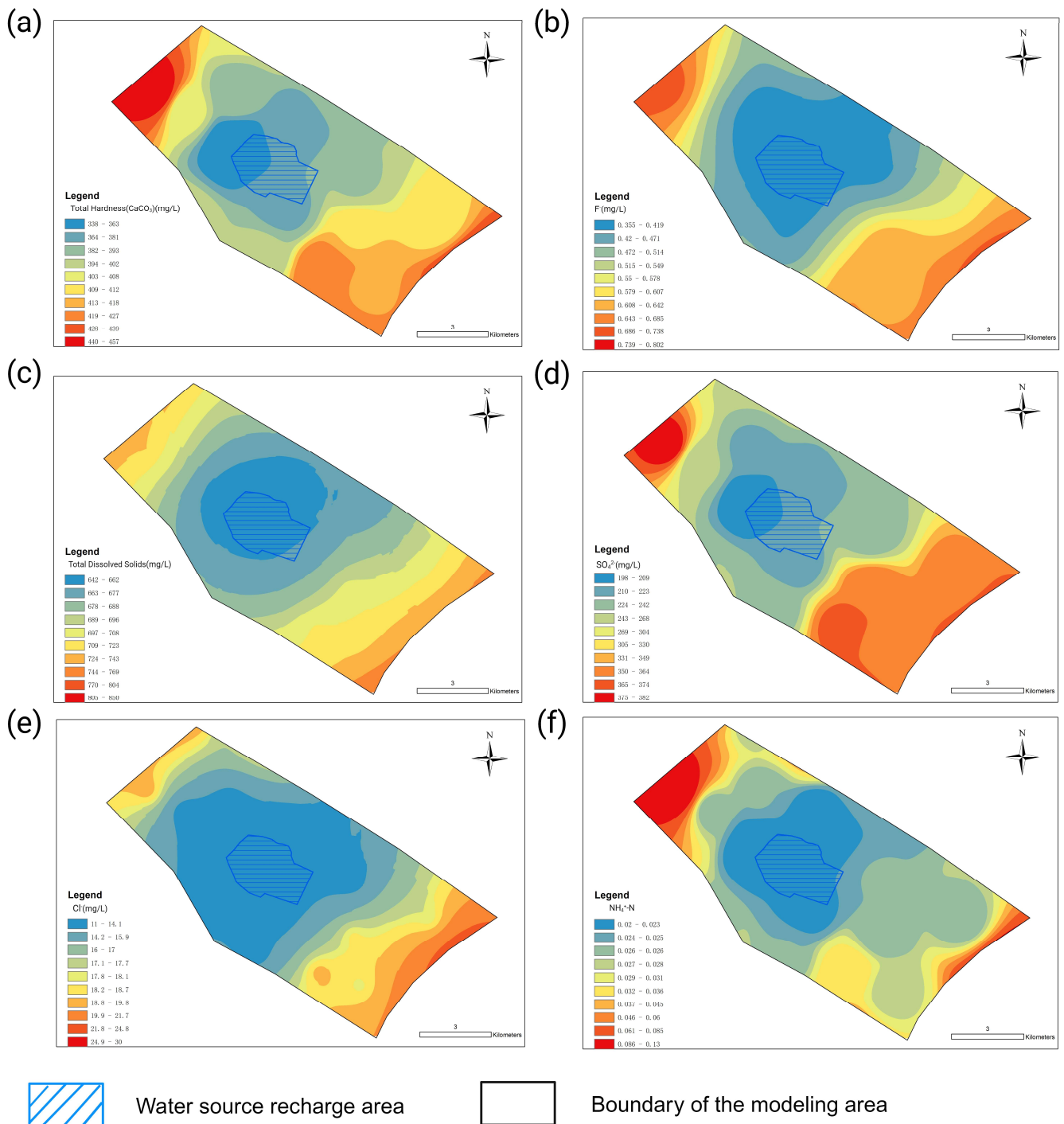


Figure 6. Tumen water source chemical element concentration spatial distribution map: (a) total hardness (CaCO₃), (b) F⁻, (c) TDS, (d) SO₄²⁻, (e) Cl⁻, and (f) NH₄⁺-N.

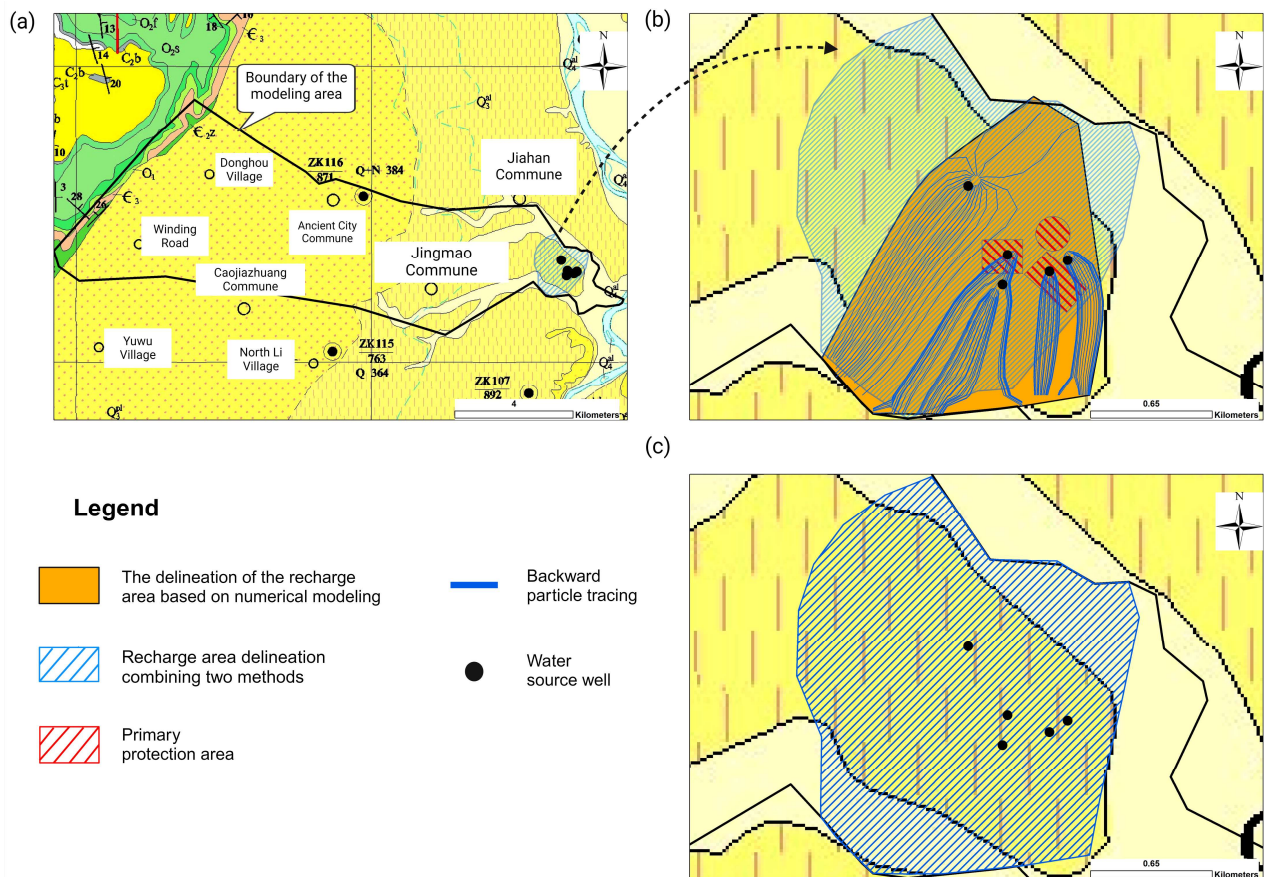


Figure 7. Hexi water source recharge area range: (a) recharge area range delineated by combining two methods; (b) comparison of numerical simulation results with those obtained from the first two methods; (c) water source recharge area range determined by the combined use of coupled methods and numerical simulation.

The numerical simulation division results (Figure 7b) indicate that the recharge area's area is smaller than that determined by the formula and hydrogeological analysis. Considering the hydraulic connection between the shallow groundwater in Sanguanyu and Huoduyu and the water source, the results from the formula and hydrogeological analysis are thoughtfully amalgamated with the numerical simulation results to discern the recharge area of the Hexi water source (Figure 7c). The final results reveal that the recharge area of the Hexi water source boasts a perimeter of 6.314 km and a total area of 2.633 km². After deducting the area of the first-level protection zone, the actual area of the recharge area is precisely 2.5224 km².

Drawing upon the water quality monitoring data from July 2020 for the Hexi water source and selectively incorporating data from other months in the same year, a comprehensive evaluation is conducted in accordance with the "Groundwater Quality Standard" (in China). The water quality of the Hexi water source is systematically categorized as class III to V groundwater, adhering to the class III water quality standard limit values. The average concentrations of the exceeded elements, i.e., total hardness, and sulfates are 514.12 mg/L and 189 mg/L, respectively. The distribution characteristics of total hardness and sulfates are conspicuously identical (Figure 8a,d). Being situated downstream in this hydrogeological unit, as the Hexi water source approaches the Fen River, the particle composition of the loose layer gradually becomes finer, obstructing the flow of groundwater and resulting in a more sluggish circulation. The total hardness and sulfates register higher values, indicative of a chemical type characterized by SO_4^{2-} - HCO_3^- -Ca·Mg. Other selected indicators, resembling those of the Tumen water source, encompass total dissolved

solids ranging from 723 to 981 mg/L, chlorides from 80.7 to 164 mg/L, fluorides from 0.22 to 0.9 mg/L, and ammonia nitrogen from 0.025 to 0.13 mg/L. The spatial distribution map of these characteristics illustrates that despite the presence of exceeded elements in the area, the water quality around the delineated recharge area persists as relatively commendable when considering all three perspectives. Therefore, this robustly affirms the rationality of the delineated recharge area results.

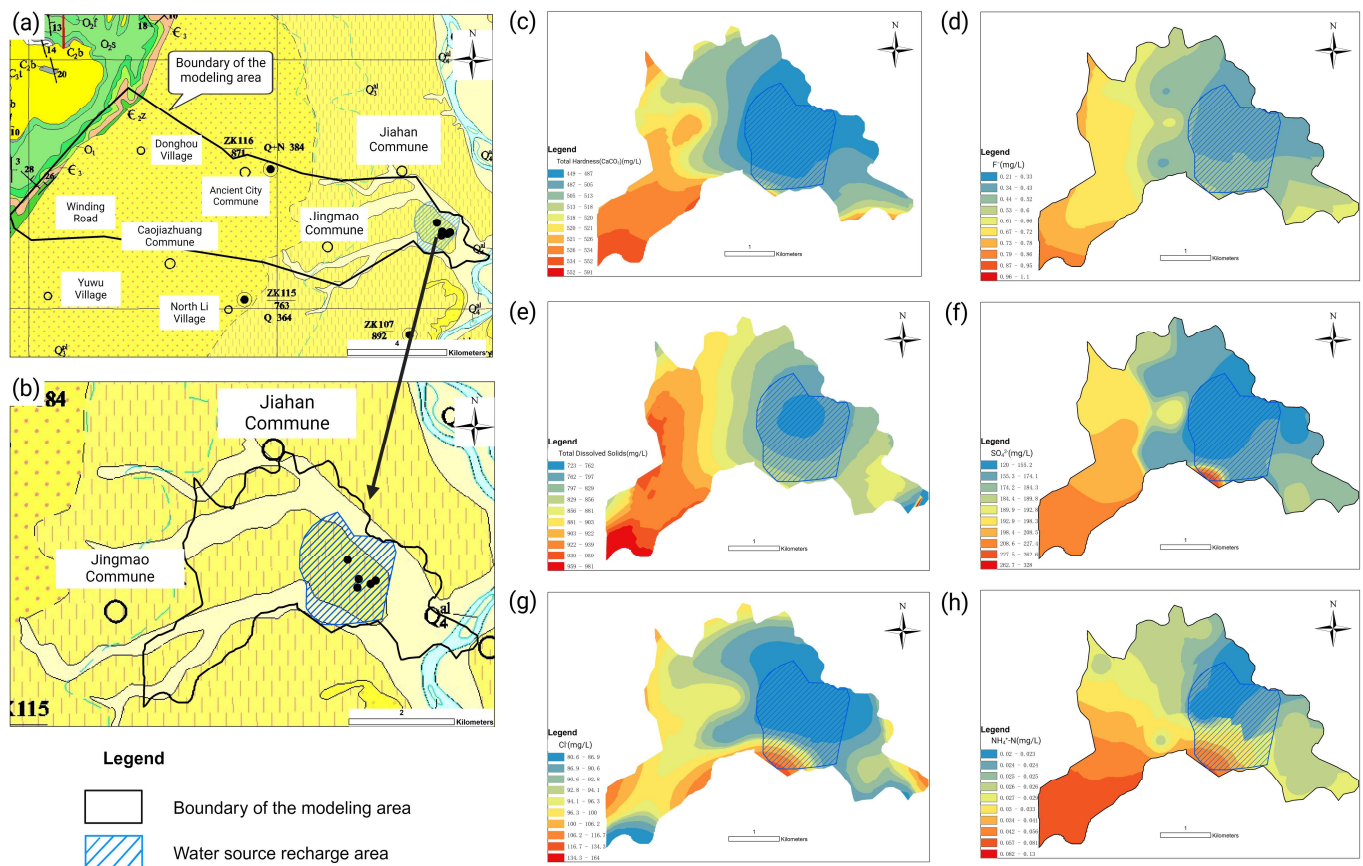


Figure 8. Chemical element concentration spatial distribution map of Hexi water source area: (a) location map of Hexi water source area; (b) GIS spatial interpolation range. (c) Total hardness (CaCO₃), (d) F⁻, (e) TDS, (f) SO₄²⁻, (g) Cl⁻, and (h) NH₄⁺-N.

3.3. Caojiapo Water Source Area Recharge Zone Division and GIS Statistical Analysis

The karst water supply to the Caojiapo water source originates from diverse pathways [41]. Some of it arises from atmospheric precipitation in the regions of Er Feng Mountain, Sikong Mountain, and Fuling Mountain, while another fraction is a result of atmospheric precipitation infiltrating the exposed and covered areas of the Ordovician limestone in the Mianshan–Danzi Mountain uplift zone (Figure 9a). Despite the considerable distance of the Er Feng Mountain, Sikong Mountain, and Fuling Mountain from the Caojiapo water source, leading to an extended groundwater migration distance and being located outside the Yicheng County region, they are not designated as the recharge areas for the Caojiapo water source. In contrast, the exposed Ordovician limestone area in the Mianshan–Danzi Mountain uplift zone near the Caojiapo water source serves as a direct source of recharge for this water source. Therefore, it is imperative to delineate it as the recharge area for the Caojiapo water source. The final determined recharge area is as follows:

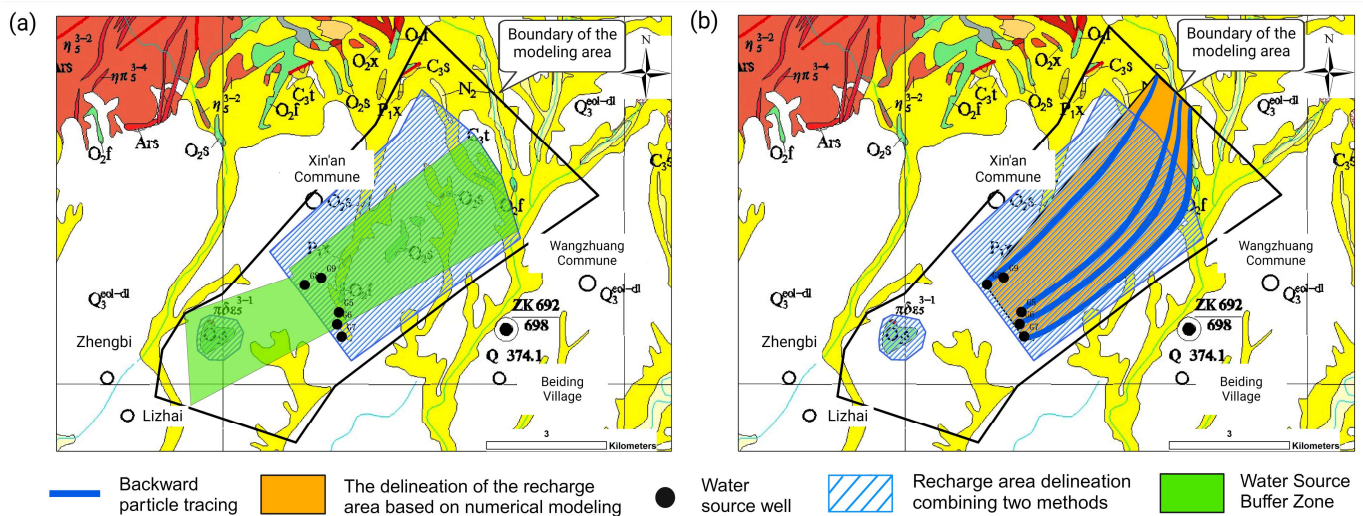


Figure 9. Caojiapo water source area recharge zone: (a) recharge zone defined by combining two methods; (b) comparison of numerical simulation results with the previous two methods.

The exposed and covered areas of the Ordovician limestone in the Mianshan–Danzi Mountain uplift zone are predominantly distributed on the mountaintops of Mianshan and Danzi Mountains and their surroundings. The exposed area and covered area of the Ordovician limestone in the Danzi Mountain, situated upstream of the groundwater flow direction, are pivotal recharge sources for the Caojiapo water source and are thus designated as the recharge area. The boundaries on the east and west sides are demarcated by the faults on both sides of the Mianshan–Danzi Mountain uplift zone, the north side by the northern boundary of the quasi-protected area, and the south side by the 150 m influence range of the water source extraction wells.

The exposed area of the Ordovician limestone in Mianshan is positioned downstream of the groundwater flow from the water source and is approximately 2.5 km away. Typically, groundwater from this section does not contribute to the water source. However, due to the peculiarities of the karst aquifer and the inclusion of this section in the quasi-protected area during the earlier delineation of the water source protection zone, it is also included as part of the recharge area.

While the application of numerical models creates challenges related to the generalized uncertainty of karst aquifers, leading to significant disparities from the recharge area results obtained by the formula and hydrogeological analysis, the overall trend demonstrates a similarity between the results from the numerical model and those from the formula and hydrogeological analysis (Figure 9b). With more detailed data, further optimization of simulation results is feasible. In summary, the results obtained using the formula and hydrogeological analysis indicate that the recharge area for the Caojiapo water source has a perimeter of approximately 22.5 km and a total area of 22.33 km². After deducting the area of the first-level protection zone, the actual recharge area is 22.29 km².

According to the single-index assessment of the groundwater quality, the water quality category for most months in the Caojiapo water source from January to December 2020 is primarily class IV or class V. The exceeded factors include the total hardness, dissolved solids, sulfate, and fluoride (Figure 10a–d). Total hardness ranges from 516 to 550 mg/L, dissolved solids exceed 797 to 1458 mg/L, sulfate ranges from 393 to 552 mg/L, and fluoride ranges from 0.9 to 1.5 mg/L. After investigation, it was found that there are no heavily polluting industries, production emissions, key pollution sources, or storage/use of toxic substances within the working area and its vicinity of the water source. The land use in the first-level protection zone is mainly for agricultural purposes, with no industrial pollution, urban pollution, or major roads crossing the area. The analysis reveals that the water source is situated in a runoff area, and during the groundwater recharge/runoff excretion process,

the prolonged interaction between the groundwater and rock formations leads to elevated levels of specific indicators. Additionally, the infiltration of atmospheric precipitation introduces soil pollutants with higher background concentrations into the groundwater, resulting in elevated levels of total hardness, sulfate, dissolved solids, and fluoride in the Caojiapo water source. The spatial distribution results of concentration characteristics show that compared to other areas in the working zone, the water quality concentration within the recharge area delineated by combining the formula and hydrogeological analysis is relatively lower, indicating the reliability of the recharge area delineation results to some extent.

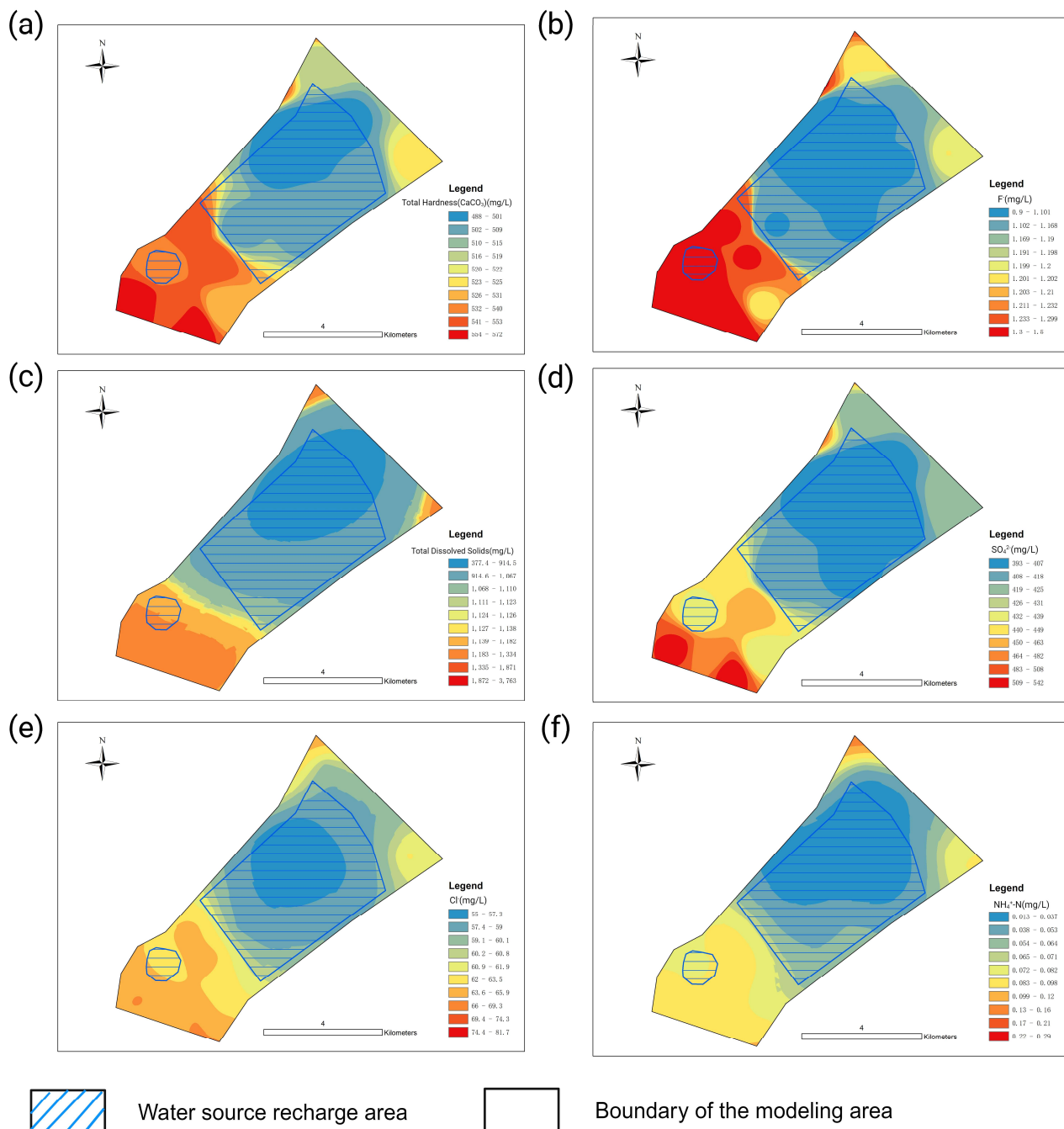


Figure 10. Chemical element concentration spatial distribution map of Caojiapo water source area: (a) total hardness (CaCO₃), (b) F⁻, (c) TDS, (d) SO₄²⁻, (e) Cl⁻, and (f) NH₄⁺-N.

4. Discussion

This research underscores the efficacy of an integrated approach, combining formulaic methodologies, hydrogeological analysis, and numerical modeling in delineating recharge areas. The discrepancies observed in numerical models underscore the challenges associated with the generalized representations of karst aquifers. The incorporation of a GIS statistical analysis augments our understanding of the spatial distribution of water quality parameters, reinforcing the reliability of recharge area delineation.

We initially delineated the recharge area using a coupled approach that combines hydrogeological analysis and formula-based methods. Subsequently, a numerical simulation method, MODPATH particle tracking, was employed for the same purpose. The previous sections provided a detailed exposition of the delineation processes for both methods, taking the Tumen and Hexi source area as examples. Both of these areas fall under the category of the fourth series, loose-type, piedmont alluvial fan source area. As depicted in Figures 5b and 7b, it is evident that the recharge area results obtained through the coupled approach and numerical simulation exhibit a certain degree of similarity in extension and trend. Moreover, there is partial overlap in certain regions. The reason for such outcomes lies in the project's initial plan to delineate the recharge areas based on the methods outlined in the guidelines [36]. However, the practical implementation revealed that the standalone use of a hydrogeological analysis or formula-based methods leads to excessively large or small areas for hydrogeological units [2]. Especially for small- to medium-sized source areas where detailed data are lacking, the use of numerical simulation methods is not recommended [12]. Furthermore, the hydrogeological analysis method is susceptible to subjective influences [4,5]. Therefore, we first employed a coupled approach using a hydrogeological analysis and formula-based methods to delineate the recharge area. Building on the identified hydrogeological units with the source area supply well as the center, we calculated the influence radius using formula-based methods [2,3]. We selected prominent features as the boundaries of the recharge area and used the numerical model to validate the accuracy of this approach. The results indicated regularity and similarity in the trends between the coupled approach and numerical simulation method in delineating the area. However, the construction of the numerical model is inevitably affected by data limitations, which can impact the accuracy of the model's delineation results. To address this, we calculated the sum of the areas delineated by the two methods and deducted the redundantly calculated areas. By analyzing the surrounding hydrogeological conditions, we refined the results obtained through numerical simulation. For instance, during the field investigations, we discovered that the northwestern boundary of the Tumen source area was an impermeable bedrock fault. Despite this, the numerical model still included this portion of the area. In response, we adopted the boundary determined by the coupled method as the boundary for the source's recharge area. This approach ensures that the delineated recharge area meets the required criteria while incorporating the local realities. The Caojiapo source area belongs to the exposed karst type, with wells extracting deep-seated karst groundwater, as detailed in the preceding sections. The numerical simulation method relies solely on particle travel time to delineate the recharge area. However, the field investigations, combined with local hydrogeological conditions, revealed that the spring's recharge sources extend to exposed areas and cover zones a certain distance upstream from the well. Consequently, in the process of delineating the recharge area for this spring (Figure 9b), we did not merely sum the areas delineated by the formula-based and numerical simulation methods. Instead, considering the special characteristics of the karst aquifer, we incorporated the exposed areas and cover zones in the mountains outside the source area into the recharge area. This study is not a straightforward application of the guidelines, but rather a pragmatic integration of different methods during practical implementation, ensuring that the research results are both reasonable and scientifically sound.

In 2021, the Chinese government promulgated the "14th Five-Year Plan for Soil, Groundwater, and Rural Ecological Environmental Protection." This plan [42] accentuates the safeguarding of recharge areas for groundwater sources supplying drinking water. It

proposes measures to refine the delineation of these areas, conduct comprehensive investigations and assessments, and advance the establishment of protection zones for urban groundwater sources, aiming to strengthen the management of the groundwater environment within these recharge zones. Subsequently, in May 2022, the Ministry of Ecology and Environment of the People's Republic of China issued the "Technical Guidelines for Delineation of Recharge Areas for Groundwater-based Drinking Water Sources (Trial)," [36] marking the initiation of delineating the recharge zones for small- to medium-sized water sources based on the delineation of water source protection zones. Our research project, initiated in June 2023, appears to be among the first to apply these guidelines. Consequently, there might be limited reference cases available at present. During field investigations, we observed a lack of groundwater level monitoring in some small- to medium-sized water sources, particularly in fractured and karst-type water sources where such monitoring is practically nonexistent. The absence of groundwater level data hinders the determination of the lateral recharge contributions from mountainous areas and leakage contributions from river boundaries. Additionally, the scarcity of borehole data in these smaller research areas poses challenges in parameter zoning. Parameters such as the hydraulic conductivity (K), specific yield (Sy), and specific storage (Ss) are primarily derived from empirical studies or a limited dataset of borehole information. Concerning the construction of the geological structure model, the obtained digital elevation model (DEM) data have an accuracy of 90 m, which is converted to 100 m using QGIS and SWAP for grid partitioning. Vertical stratification relies on a handful of borehole data to roughly estimate the depths of the unconfined and confined aquifers. Furthermore, the rainfall and evaporation data are calculated based on annual averages, considering the lack of more granular data. Nevertheless, the currently established, steady-state numerical model provides valuable insights for delineating recharge areas. Therefore, we recommend, as part of the National Groundwater Monitoring Project, the installation of groundwater monitoring wells for all drinking water sources. Conforming to relevant standards, the regular monitoring of groundwater levels can significantly improve the accuracy of the model. This enhancement would result in a more precise delineation of recharge zones through numerical simulations, thereby ensuring that the model's computational and predictive outcomes are both scientifically sound and reasonable.

5. Conclusions

This comprehensive study successfully delineated water source recharge area boundaries for the Tumen, Hexi, and Caojiapo drinking water sources in Linfen City, China. Adhering to relevant technical specifications, including the "Technical Guidelines for Delineation of Water Source Recharge Areas for Underground Drinking Water," the research adopted a meticulous approach based on the hydrogeological conditions of each area. The delineation process integrated empirical formula methods, hydrogeological unit analyses, and numerical simulations, establishing a robust foundation for the results.

- (1) For the Tumen water source, the combination of formula-based methods and a hydrogeological analysis, validated through numerical modeling, delineated a recharge area of 5.5 km², inclusive of a protective buffer zone. The chemical analysis affirmed that groundwater within this delineated area adhered to class III groundwater standards, reinforcing the rationality of the recharge area determination.
- (2) The Hexi water source's recharge area, determined through formulaic and hydrogeological approaches with numerical validation, covered 2.5224 km², incorporating a protective buffer zone. The water quality assessments indicated groundwater ranging from class III to V, with specific constituents exceeding permissible limits. Notably, the GIS statistical analysis revealed that the defined recharge area maintained a relatively better water quality despite localized exceedances.
- (3) The delineation of the Caojiapo water source recharge area, considering the nuances of karst water sources, showcased consistency among the formula-based, hydrogeological, and numerical methods. The delineated area, totaling 22.29 km² after deducting

the protected zone, was supported by a chemical analysis indicating groundwater exceeding permissible limits. The spatial distribution analysis revealed localized exceedances, emphasizing the overall comparatively better water quality within the defined recharge area.

In conclusion, this research offers valuable insights into the delineation of water source recharge areas, providing a nuanced understanding of each area's hydrogeological conditions and contributing to effective groundwater protection strategies in Linfen City. The results establish a foundation for sustainable water resource management, ensuring the continued availability of high-quality drinking water from these sources.

Author Contributions: Conceptualization, J.S., Q.Z. and Y.C.; methodology, K.L.; software, K.L.; validation, K.L., Q.Z., Y.C., J.S., Y.Z. (Yaobin Zhang), Y.Z. (Yan Zhou), and Y.D.; writing—original draft preparation, K.L., Y.D. and J.S.; writing—review and editing, J.S., Q.Z., Y.C., K.L., Y.Z. (Yaobin Zhang), Y.Z. (Yan Zhou), and Y.D.; supervision, Q.Z., Y.C. and J.S.; project administration, Q.Z., Y.C., L.L. and J.S. All authors have read and agreed to the published version of the manuscript.

Funding: This research was financially supported by the projects of the Linfen Ecology and Environment Bureau (No. JF20220353).

Institutional Review Board Statement: Not applicable.

Informed Consent Statement: Not applicable.

Data Availability Statement: The datasets generated and analyzed during the current study are available from the corresponding author upon reasonable request.

Acknowledgments: The authors would like to thank the Third Geological Engineering Exploration Institute of Shanxi Province for their research data.

Conflicts of Interest: Author Lu Lyu was employed by the company The Third Geological Engineering Exploration Institute of Shanxi Province. The remaining authors declare that the research was conducted in the absence of any commercial or financial relationships that could be construed as a potential conflict of interest.

References

- Li, J. The Establishment and Protection of Drinking Water Resource Protection Areas in Germany. *Adv. Geogr.* **1998**, *4*, 90–99.
- Xu, H.; Li, G.; Zhang, S.; Dong, Y. A Review of Methods for Division of Groundwater Source Protection Areas. *Adv. Sci. Technol. Water Resour.* **2009**, *29*, 80–84.
- U.S. Environmental Protection Agency. *Ground Water and Wellhead Protection Handbook*; EPA-625/R-94-001; U.S. Environmental Protection Agency, Office of Water: Washington, DC, USA, 1994.
- Thomsen, R.; Søndergaard, V.H.; Sørensen, K.I. Hydrogeological Mapping as a Basis for Establishing Site-Specific Groundwater Protection Zones in Denmark. *Hydrogeol. J.* **2004**, *12*, 550–562. [[CrossRef](#)]
- Gemitzi, A.; Petalas, C.; Tsihrintzis, V.A.; Pisinaras, V. Assessment of Groundwater Vulnerability to Pollution: A Combination of GIS, Fuzzy Logic and Decision Making Techniques. *Environ. Geol.* **2006**, *49*, 653–673. [[CrossRef](#)]
- Shan, C. An Analytical Solution for the Capture Zone of Two Arbitrarily Located Wells. *J. Hydrol.* **1999**, *222*, 123–128. [[CrossRef](#)]
- De Smedt, F. Analytical Solution for Capture and Catchment Zones of a Well Located on a Groundwater Divide: Technical Note. *Water Resour. Res.* **2014**, *50*, 736–740. [[CrossRef](#)]
- De Smedt, F. Analytical Solution for the Catchment Zone of a Well Located near a Groundwater Divide in a Recharged Semi-Confined Aquifer. *J. Hydrol.* **2014**, *519*, 1271–1277. [[CrossRef](#)]
- Javandel, I.; Tsang, C. Capture-Zone Type Curves: A Tool for Aquifer Cleanup. *Groundwater* **1986**, *24*, 616–625. [[CrossRef](#)]
- Grubb, S. Analytical Model for Estimation of Steady-State Capture Zones of Pumping Wells in Confined and Unconfined Aquifers. *Groundwater* **1993**, *31*, 27–32. [[CrossRef](#)]
- Intaraprasong, T.; Zhan, H. Capture Zone between Two Streams. *J. Hydrol.* **2007**, *338*, 297–307. [[CrossRef](#)]
- Anderson, M.P.; Woessner, W.W.; Hunt, R.J. *Applied Groundwater Modeling: Simulation of Flow and Advective Transport*, 2nd ed.; Academic Press: London, UK; San Diego, CA, USA, 2015; ISBN 978-0-12-058103-0.
- Pollock, D.W. *User's Guide for MODPATH/MODPATH-PLOT, Version 3: A Particle Tracking Post-Processing Package for MODFLOW*; The U.S. Geological Survey Finite-Difference Ground-Water Flow Model, USGS Pubs Warehouse: Reston, VA, USA, 1994.
- Wuol, R.W.; Dahlstrom, D.J.; Fairbrother, M.D. Wellhead Protection Area Delineation Using the Analytic Element Method of Ground-Water Modeling. *Groundwater* **1995**, *33*, 71–83. [[CrossRef](#)]

15. Dong, Y.; Xu, H.; Li, G. Wellhead Protection Area Delineation Using Multiple Methods: A Case Study in Beijing. *Environ. Earth Sci.* **2013**, *70*, 481–488. [[CrossRef](#)]
16. Taylor, J.Z.; Person, M. Capture Zone Delineations on Island Aquifer Systems. *Groundwater* **1998**, *36*, 722–730. [[CrossRef](#)]
17. Todd, D.K. *Groundwater Hydrology*, 2nd ed.; John Wiley: New York, NY, USA, 1980.
18. Bear, J.; Jacobs, M. On the Movement of Water Bodies Injected into Aquifers. *J. Hydrol.* **1965**, *3*, 37–57. [[CrossRef](#)]
19. Paradis, D.; Martel, R.; Karanta, G.; Lefebvre, R.; Michaud, Y.; Therrien, R.; Nastev, M. Comparative Study of Methods for WHPA Delineation. *Groundwater* **2007**, *45*, 158–167. [[CrossRef](#)] [[PubMed](#)]
20. Hanson, R.T.; Kauffman, L.K.; Hill, M.C.; Dickinson, J.E.; Mehl, S.W. *Advective Transport Observations with MODPATH-OBS Documentation of the MODPATH Observation Process*; U.S. Geological Survey Technology: Sunrise Valley Drive Reston, VA, USA, 2013; p. 94.
21. Neupauer, R.M.; Wilson, J.L. Adjoint Method for Obtaining Backward-in-time Location and Travel Time Probabilities of a Conservative Groundwater Contaminant. *Water Resour. Res.* **1999**, *35*, 3389–3398. [[CrossRef](#)]
22. Neupauer, R.M.; Wilson, J.L. Adjoint-derived Location and Travel Time Probabilities for a Multidimensional Groundwater System. *Water Resour. Res.* **2001**, *37*, 1657–1668. [[CrossRef](#)]
23. Neupauer, R.M.; Wilson, J.L. Backward Location and Travel Time Probabilities for a Decaying Contaminant in an Aquifer. *J. Contam. Hydrol.* **2003**, *66*, 39–58. [[CrossRef](#)]
24. Chin, D.A.; Chittaluru, P.V.K. Risk Management in Wellhead Protection. *J. Water Resour. Plann. Manag.* **1994**, *120*, 294–315. [[CrossRef](#)]
25. Fadlelmawla, A.A.; Dawoud, M.A. An Approach for Delineating Drinking Water Wellhead Protection Areas at the Nile Delta, Egypt. *J. Environ. Manag.* **2006**, *79*, 140–149. [[CrossRef](#)]
26. Rock, G.; Kupfersberger, H. Numerical Delineation of Transient Capture Zones. *J. Hydrol.* **2002**, *269*, 134–149. [[CrossRef](#)]
27. Festger, A.D.; Walter, G.R. The Capture Efficiency Map: The Capture Zone Under Time-Varying Flow. *Groundwater* **2002**, *40*, 619–628. [[CrossRef](#)] [[PubMed](#)]
28. Abelardo, R.-P.; Nowak, W. Integrating Transient Behavior as a New Dimension to WHPA Delineation. *Adv. Water Resour.* **2018**, *119*, 178–187. [[CrossRef](#)]
29. Feyen, L.; Beven, K.J.; De Smedt, F.; Freer, J. Stochastic Capture Zone Delineation within the Generalized Likelihood Uncertainty Estimation Methodology: Conditioning on Head Observations. *Water Resour. Res.* **2001**, *37*, 625–638. [[CrossRef](#)]
30. Feyen, L.; Gómez-Hernández, J.J.; Ribeiro, P.J.; Beven, K.J.; De Smedt, F. A Bayesian Approach to Stochastic Capture Zone Delineation Incorporating Tracer Arrival Times, Conductivity Measurements, and Hydraulic Head Observations. *Water Resour. Res.* **2003**, *39*, 2002WR001544. [[CrossRef](#)]
31. Sousa, M.R.; Frind, E.O.; Rudolph, D.L. An Integrated Approach for Addressing Uncertainty in the Delineation of Groundwater Management Areas. *J. Contam. Hydrol.* **2013**, *148*, 12–24. [[CrossRef](#)] [[PubMed](#)]
32. Frind, E.O.; Molson, J.W. Issues and Options in the Delineation of Well Capture Zones under Uncertainty. *Groundwater* **2018**, *56*, 366–376. [[CrossRef](#)]
33. Okkonen, J.; Neupauer, R.M. Capture Zone Delineation Methodology Based on the Maximum Concentration: Preventative Groundwater Well Protection Areas for Heat Exchange Fluid Mixtures. *Water Resour. Res.* **2016**, *52*, 4043–4060. [[CrossRef](#)]
34. Bjerre, E.; Kristensen, L.S.; Engesgaard, P.; Højberg, A.L. Drivers and Barriers for Taking Account of Geological Uncertainty in Decision Making for Groundwater Protection. *Sci. Total Environ.* **2020**, *746*, 141045. [[CrossRef](#)]
35. Sbaji, M.A. A Dual Delineation Approach to Untangle Interferences in Well Doublets Systems. *Groundwater* **2020**, *58*, 822–830. [[CrossRef](#)]
36. Ministry of Ecology and Environment of the People’s Republic of China. *Technical Guidelines for Delineation of Groundwater Drinking Water Source Recharge Areas (Trial)*; Ministry of Ecology and Environment of the People’s Republic of China: Beijing, China, 2022. (In Chinese)
37. McCuen, R.H. *Modeling Hydrologic Change: Statistical Methods*; CRC Press: Boca Raton, FL, USA, 2002; ISBN 978-0-429-14317-5.
38. GB/T 14848-2017; Groundwater Quality Standard. Standards Press of China: Beijing, China, 2017. (In Chinese)
39. Duan, X.D.; Li, H.M.; Qiu, Y.Q.; Xiao, H.; Lv, X.L.; Dong, H.; Zheng, H. Numerical Simulation Study on Dynamic Changes in Groundwater Level in Linfen Basin. *Water Hydropower Energy Sci.* **2023**, *41*, 15–18+10. [[CrossRef](#)]
40. China Geological Survey. *Handbook of Hydrogeology*, 2nd ed.; Geological Publishing House: Beijing, China, 2012; ISBN 978-7-116-07785-0. (In Chinese)
41. Shen, H.; Liang, Y.; Zhao, C.; Tang, C.; Wang, Z. Hydro-Geological Characteristics and Demarcation of Gudui Spring Karst Groundwater System. *J. Jilin Univ.* **2020**, *50*, 217–225. [[CrossRef](#)]
42. Ministry of Ecology and Environment of People’s Republic of China. *Soil, Groundwater and Rural Ecological Environment Protection Plan under the 14th Five-Year Plan*; Central People’s Government of the People’s Republic of China: Beijing, China, 2022. (In Chinese)

Disclaimer/Publisher’s Note: The statements, opinions and data contained in all publications are solely those of the individual author(s) and contributor(s) and not of MDPI and/or the editor(s). MDPI and/or the editor(s) disclaim responsibility for any injury to people or property resulting from any ideas, methods, instructions or products referred to in the content.